

CANGAROO RESULTS ON SOUTHERN SKY TEV GAMMA-RAY SOURCES

Toru Tanimori

Department of Physics, Graduate School of Science,
Kyoto University, Kyoto, Japan, 606-8502

On behalf of the CANGAROO Collaboration

ABSTRACT

The Cangaroo group has been observing TeV gamma-ray sources with its air Čerenkov telescopes at Woomera, Australia since 1992. The southern sky provides good chance to observe Galactic objects such as supernova remnants (SNR's), pulsars/pulsar nebulae, and stellar-size black holes. SNR's are particularly interesting targets because they have been most promising origins of cosmic rays throughout history of cosmic ray physics. Detection of high-energy gamma rays will give a strong evidence for this belief and lead to understanding of the acceleration mechanism at shock fronts of SNR's.

In this presentation, I will devote most of my time to observational results on two SNR's and the rest to information about particle acceleration at SNR's obtained in multi-wavelength observations.

1 Introduction

GeV gamma-ray astronomy was established in 1990's. The Compton Gamma-Ray Observatory(CGRO) was launched in 1991,¹ which covered a wide range of gamma-ray energy from sub-MeV to GeV regions by four detectors (BATSE, OSSE, COMPTEL and EGRET). EGRET was a detector observing sub-GeV and GeV high-energy gamma rays on-board CGRO, and found about 270 gamma-ray point sources. About one thirds are of extra-galactic origin. About two thirds of the sources are considered Galactic origin, such as pulsars/pulsar nebulae and SNR's, although the most of those sources are still unidentified.

TeV gamma-ray astronomy was also raised in the same decade. Several TeV gamma-ray sources have been firmly detected: Crab pulsar/nebula,² Mrk421,³ Mrk501,⁴ PSR1706-44.⁵ Celestial objects emitting TeV gamma rays had been expected as a natural consequence of the existence of cosmic rays, and have been searched since 1960's using ground-based detectors, such as scintillation-counter arrays and air Čerenkov telescopes. Nevertheless, due to huge background of hadron showers overwhelming the tiny signal of celestial gamma rays, no persistent TeV gamma-ray source was found until the discovery of TeV gamma-ray emission from the Crab by the Whipple group in 1989.² The Whipple group developed an imaging Čerenkov technique,⁶ and hence the rejection power of hadron showers was greatly improved. In the 1990's several types of TeV gamma-ray sources were detected with high statistics by adopting this imaging technique. In particular, successive discoveries of AGN emitting TeV gamma rays were astonishing.^{3,4} A good review that includes recent interesting results of AGNs was presented at this conference by Dr. F.Krennich.

Our group, CANGAROO, a collaboration of Japanese and Australian institutes, has observed TeV gamma-ray sources in the southern hemisphere since 1992 in South Australia.⁷ The southern hemisphere provides a good chance to observe many Galactic objects, such as pulsar/nebulae, SNR's, black holes, and the Galactic center. We have found several Galactic TeV gamma ray sources, as listed in a review article of Weekes.⁸ In particular, recent noteworthy discoveries are several reports on the detection of TeV gamma-ray emissions from shell-type SNR's in both southern and northern skies,⁹⁻¹¹ of which two SNR's were detected by CANGAROO.

Before talking about our results of SNR's, I have to point out something about the extra-galactic sources in the southern hemisphere. All of the observed targets by CANGAROO telescopes are summarized in Table1. You might note that CANGAROO

has observed many extra-galactic sources as well as Galactic objects. Especially, we have the merit of being able to observe nearby galaxies. As is well known, two nearest ones, the Large and Small Magellanic Clouds, can be seen only from the southern hemisphere. In addition, famous star-burst galaxy NGC253, and the nearest radio galaxy, Cen-A, also are located. Actually, last year CANGAROO reported the detection of TeV gamma rays from NGC253.¹²

2 Cosmic-ray origin and shock acceleration

For a long time, SNR's have been believed to be a favored site for accelerating cosmic rays up to 10^{15} eV, because they look to satisfy the required energy input rate to the galaxy among several Galactic objects.¹³ In addition, a shock acceleration theory was established around 1980s, in which particles are accelerated from the interaction between particles and collective motion of the plasma fluid moving at a supersonic velocity in space.¹⁴ SNR's are just an extended and heated gas system accompanying very strong shocks. Shocks are very common phenomena in the universe, and hence shock acceleration has been widely applied to high-energy phenomena in the universe. Thus, the shock-acceleration mechanism has been a standard theory for particle acceleration in astrophysics. Although this theory looks very simple and reliable, an observational evidence is still very sparse.

In order to investigate the shock-acceleration mechanism, SNR is an unique and ideal laboratory because it is quite simple and a well-understood astronomical object. The evolution of an SNR can be fairly well explained with several observable parameters, such as the explosion energy of an SNR, the total mass of the ejecta, the density of the inter-stellar medium (ISM) around the SNR and the age after the explosion.¹⁵ In addition, the resolvable size of an SNR enables us to directly observe the geometrical structure of the shock front accelerating particles, which provides many significant physical parameters quantitatively (absolute value of the magnetic field, index of the power law, maximum energy of particle acceleration).

If particles are accelerated in the universe, several radiative emissions are expected.¹⁶ Although both electrons and protons (or ions) are accelerated, almost all non-thermal emissions in the universe are ascribed to those by only accelerated electrons. Since a magnetic field of $\sim \mu$ Gauss is considered to exist in any space region of galaxies and halos, high-energy electrons emit synchrotron radiation from radio to X-ray everywhere: GeV electrons emit radio waves mainly and 100 TeV ones emit X-rays. High-energy

Table 1: Objects observed with the CANGAROO-III telescope from March 2000 to April 2003.

Object [†]	<i>d</i> (kpc)	ON-source obs. (hr) [‡]				Status [#]
		2000	'01	'02	'03	
SNR						
RXJ 0852.0–4622 ^a	0.5	-	-	41	51	A
SN1006 ^a (NE rim)	2	52	33	-	43	D*
RCW86 ^a (SW shell)	3 (1)	-	38	41	65	A
RX J1713.7–3946 ^a	6 (1)	-	24	44	-	D*
SN1987A ^a	50	-	21	-	-	U
Pulsar/Nebula						
Vela ^b	0.25	12	39	38	-	A
PSR B1706–44 ^b	1.8	32	31	-	-	D*
Crab ^b	2.0	55	-	-	-	D*
PSR 1509–58 ^b	4.2	-	-	35	-	A
PSR J1420–6048 ^b	7.7 (2)	-	-	26	-	A
PSR 1259–63 ^c	1.5	3	18	-	-	U
Another Galactic Objects						
SS 433 ^d (W lobe)	5	-	51	34	-	A
Sgr A* ^e	8	-	52	82	-	A
Nearby Galaxies						
SMC ^f	64	-	-	41	-	A
NGC 253 ^g	2.5 Mpc	38	43	-	-	D
Active Galactic Nuclei						
Mrk 421 ^h	$z = 0.031$	-	18	9	6	D
EXO 0556.4–3838 ^h	$z = 0.034$	-	-	21	15	A
PKS 0548–322 ^h	$z = 0.069$	3	-	-	-	A
PKS 2005–489 ^h	$z = 0.071$	33	-	-	-	U
PKS 2155–304 ^h	$z = 0.116$	36	29	-	-	U
Cluster of Galaxies						
3EG J1234–1318 ⁱ	-	-	-	23	-	A

[†] ^aSNR, ^bpulsar/nebula, ^cpulsar/Be star binary, ^dmicro quasar, ^eGalactic center, ^fgalaxy in the Local Group, ^gstarburst galaxy, ^hblazar(HBL), ⁱEGRET unidentified. [‡] Bad weather runs are included. From 2000 to 2002 they were taken with a single telescope, while stereo observations have been conducted in 2003. Each observation time of OFF-source runs is roughly the same as ON-source runs. [#] A:Under analysis, D:Detected with a statistical significance exceeding 5 standard deviations, and furthermore the * symbol shows double detections with the CANGAROO-III and CANGAROO-I (3.8 m) telescopes, U:Upper limit obtained.

electrons also generate high-energy gamma rays everywhere due to the inverse Compton (IC) scattering with 2.7K Cosmic Microwave Background (CMB) or infra-red emission from a star, where scattered photons acquire an energy of about one tenth of that of the parent electrons. Then, several 10 TeV electrons generates high-energy gamma rays in the TeV region. In dense regions, high-energy electrons also emit photons over a very wide range from soft X-rays to high-energy gamma rays by the bremsstrahlung process.

As is well known, the intensity of synchrotron emission is proportional to the flux of the parent electron and the square of the strength of the magnetic field, while the intensity of gamma rays due to IC scattering with CMB is proportional to the flux of the parent electron. We know a simple but useful formula, connecting high-energy photons due to the IC process with synchrotron photons through a high-energy electron, magnetic filed and a soft seed photon. The emission intensity of synchrotron radiation and IC scattering, P_{sync} and P_{IC} , are respectively expressed as follows:

$$P_{sync} = \frac{4}{3}\sigma_T c\gamma^2 \beta^2 U_B, \quad P_{IC} = \frac{4}{3}\sigma_T c\gamma^2 \beta^2 U_{soft}, \quad (1)$$

where σ_T is the Thomson cross section, $\sigma_T = 6.7 \times 10^{-25} \text{ cm}^2$, and $c\beta$ and γ are the velocity and Lorentz factor of the electron. U_B and U_{soft} are energy densities of the magnetic field and the soft seed photons, respectively. Since the energy density of soft seed photons (CMB) is well-known, an observed gamma-ray flux provides a good estimation of the magnetic field strength at the acceleration site.

Thus, accelerated electrons surely emit some radiation signals, but accelerated protons are quite different. The mass of a proton is too heavy to emit radiations by any electromagnetic process, even if a proton is accelerated to $\geq 10^{15} \text{ eV}$. The only process in which high-energy protons emit photons is the generation of a neutral pion π^0 , which decays into two gamma rays simultaneously, due to a hard collision between a high-energy proton and the inter-stellar medium (ISM). Since the intensity of gamma rays is proportional to the density of ISM and the flux of high-energy protons, such gamma rays are only expected to be observed from a dense region. Hence, even if protons are accelerated in some celestial object, there is not so much chance to emit gamma rays from it. On the other hand, synchrotron or IC emission is quite expected from the most acceleration sites as mentioned before.

When gamma rays are detected from some celestial object, how can we identify the parent particles (electron or proton)? In particular, to verify the origin of cosmic rays, we have to obtain clear evidence of proton acceleration. Identification of the parent particles of TeV gamma rays is possible by observing the wide spectrum from the sub to

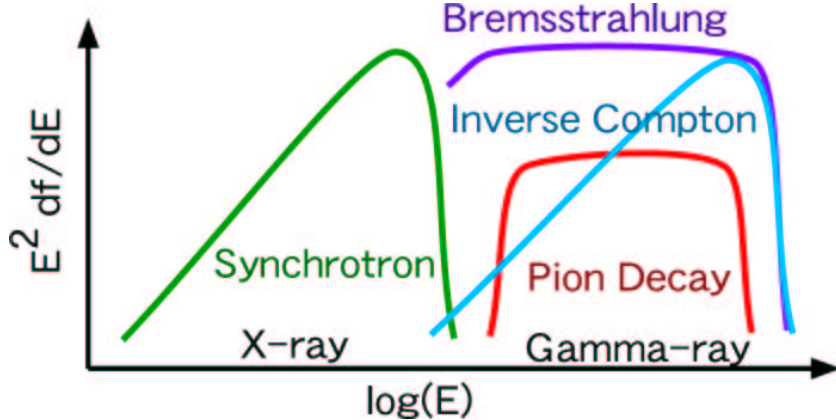


Figure 1: Schematic image of expected energy spectra from IC process, π^0 decay, and bremsstrahlung with synchrotron spectrum.

multi TeV region, as shown in Fig. 1. A gamma-ray spectrum flatter than $E^{-2.0}$ in this region is surely due to the IC process, while that due to π^0 decay generated by collisions between ISM and high-energy protons is expected to be steeper than $E^{-2.0}$. Also, the spectrum due to protons is expected to have a low-energy cut-off at around 70 MeV due to the kinematics of π^0 decay to two photons. The expected gamma-ray spectra via a bremsstrahlung process is similar to that of protons, but its spectrum is extended to the X-ray regions below 70 MeV, as shown in Fig. 1.

3 SN1006: first evidence of electron acceleration up to \geq TeV

The first evidence for very high-energy particle acceleration in an SNR was due to an observation of the strong synchrotron emission of SN1006 by the Japanese X-ray satellite ASCA in 1995.¹⁷ Until that time, thermal X-ray emissions, which are known to be emitted from the heating plasma by a shock wave, had been observed from many SNR's, whereas no confident synchrotron X-ray emission had been observed. By assuming a magnetic field of several μ Gauss, the observed synchrotron X-ray emission strongly supported the existence of high-energy electrons of tens or hundreds of TeV, which also means that such a high-energy electron simultaneously emit high-energy gamma rays via IC process with CMB. Their energies are expected to reach nearly 10 TeV in

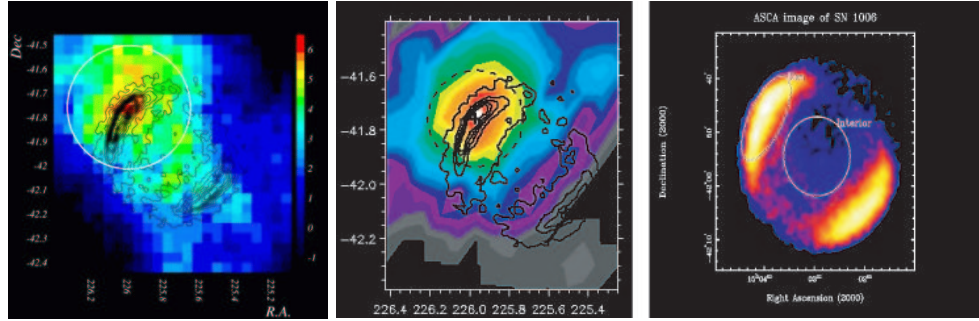


Figure 2: SN1006 images of TeV gamma-ray observed by 10m telescope (left), same one by 3.8m telescope (center) and ASCA hard X-ray (right).

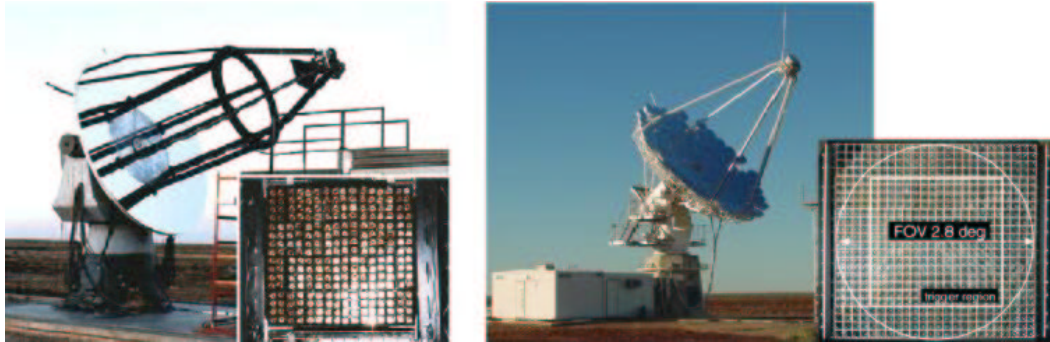


Figure 3: Photographs of 3.8 m (left) and first 10 m (right) telescopes of CANGAROO are presented with the front view of each camera.

SN1006, which could be detected by the CANGAROO telescope.^{18–21} In 1996 and 1997, CANGAROO succeeded to detect the TeV gamma-ray emission from the north rim of SN1006 using a 3.8m imaging telescope,⁹ as shown in Fig. 2. In 2000 we constructed a new 10m telescope to exploit the sub-TeV energy region, and soon SN1006 was observed again by this new telescope, as shown in Fig. 2.²² Also in Figs. 3, the photographs of 3.8 m and first 10 m telescopes of CANGAROO are presented.

Figure 4 shows the wide band energy spectrum at the north rim of SN1006 from radio to TeV, and also the fitting result based on the synchrotron-IC model,²³ where the above relation between IC and synchrotron emissions is used in principle. All data were fitted very well, and several significant parameters (magnetic field(B), power index(a), maximum energy (E_{\max})) were determined independently: $B = 4.3\mu$ Gauss, $a = 2.2$, and $E_{\max} = 60$ TeV.

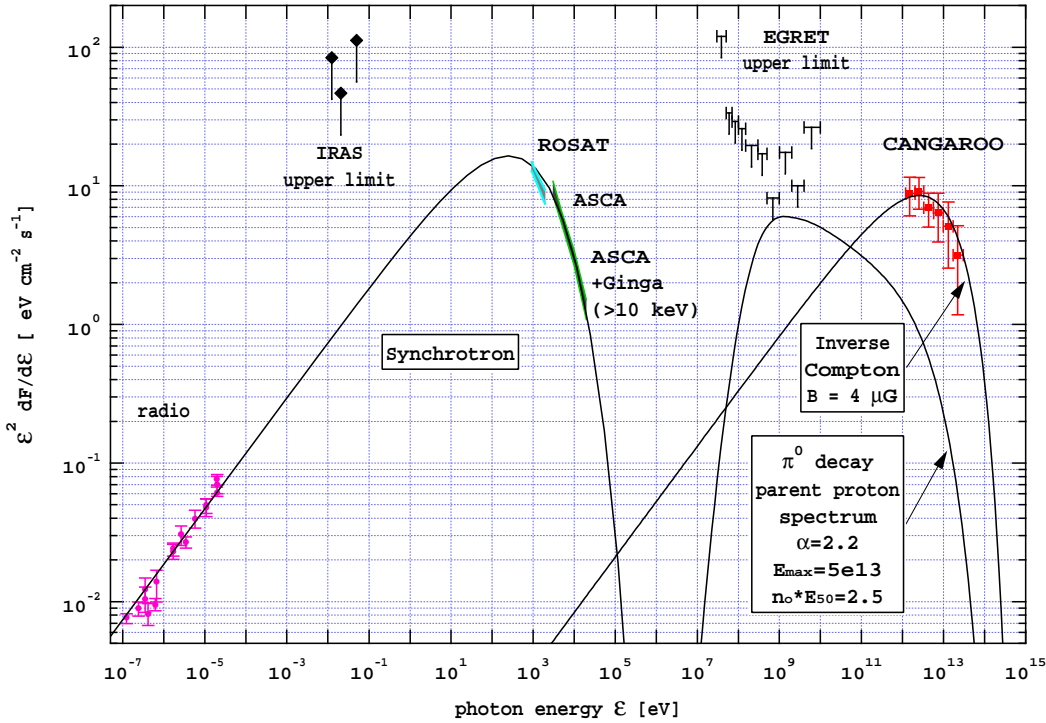


Figure 4: Energy spectrum at the north rim of SN1006 from radio to TeV, and also fitting results based on the shock model.

Here, we assumed that the detected TeV gamma-ray emission is mainly due to IC process with very high-energy electrons, considering the tenuous shell of ($\leq \sim 0.4$ cm $^{-3}$).²⁴ In fact the expected spectrum from π^0 decay can not satisfy both our data and the upper limit in the GeV region observed by EGRET (Fig.4) simultaneously.

4 RX J1713.7-3946: first evidence of proton acceleration up to the TeV region

After the discovery of synchrotron X-ray emission, several SNR's emitting synchrotron X-rays were found. RX J1713.7-3946 was observed to be the strongest synchrotron X-ray emitter among these SNR's by ASCA in 1997,²⁵ and subsequently TeV emission was detected from the maximum X-ray emission point.¹⁰ Although this SNR emits intense synchrotron X-rays like SN1006, these two SNR's look different. Its morphology is

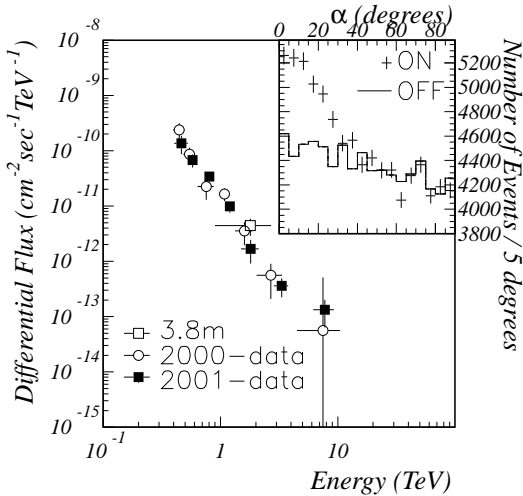


Figure 5: Differential fluxes of RX J1713.7-3946 obtained by this experiment together with that of CANGAROO-I. The inserted graph is the excess events determined from plots of the image orientation angle.

obviously more complex than that of SN1006, of which the north parts might interact with the molecular cloud observed by a radio telescope.²⁶ Therefore, this TeV emission might be ascribed to the π^0 decay generated by the collisions of accelerated protons with the molecular cloud.

To clarify the nature of the accelerated particles, we observed this point again in 2000 and 2001 using the 10 m telescope.²⁷ The result has been recently published.²⁸

The differential fluxes of TeV gamma-rays from RX J1713.7-3946 are plotted in Fig. 5 along with previous data.¹⁰ The best fit is

$$dF/dE = (1.63 \pm 0.15 \pm 0.32) \times 10^{-11} (E/1\text{TeV})^{-2.84 \pm 0.5 \pm 0.20} \text{ TeV}^{-1} \text{cm}^{-2} \text{s}^{-1}, \quad (2)$$

where the first errors are statistical and the second are systematic. The power-law spectrum increases monotonically as the energy decreases. This feature is in contrast to the TeV gamma-ray spectrum of SN 1006, which flattens below 1 TeV,²⁹ and is consistent with synchrotron/Inverse Compton (IC) models.^{18-21,23} While both SNR's emit intense X-rays via the synchrotron process, different TeV spectra suggest that different emission mechanisms may act, respectively.

The morphology of the gamma-ray emitting region is shown by the thick- solid contours in Fig. 6, together with the synchrotron X-ray ($\geq 2\text{keV}$) contours by ASCA³⁰

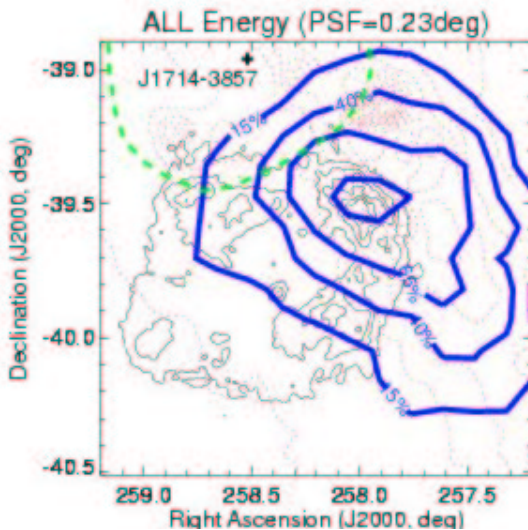


Figure 6: Revised profile of the emission of TeV gamma rays around RX J1713.7-3946 (solid thick), intensity profile of hard X-rays³⁰ (solid thin) and infrared³¹ (dotted).

and infrared ones from IRAS 100 μ m results,³¹ which possibly indicates the density distribution of the inter stellar matter. This figure has recently been modified after the publication, since a small bug in the software used to calculate the direction of observed gamma rays was found. In this figure, the observed TeV gamma-ray intensity peak coincides with the maximum point in the NW-rim observed in X-ray, but the TeV gamma-ray emission extends over the ASCA contours. In particular, a modified emission region of TeV gamma rays shows an extension toward the north-west, which is in the opposite direction to the extension of hard X-ray emission. Thus, the distribution of TeV gamma rays seems to extend towards the CO cloud in the north-west. The nearby GeV gamma-ray source EG J1714-3857, reported in the EGRET 3rd Catalog, is also plotted.¹ A recent paper pointed out the possible coincidence of this source to RX J1713.³² Here, we stress that the observed TeV gamma rays obviously emit not from this GeV source point, but from the maximum point of the hard X-ray emission, considering the uncertainty of the point-spread function of our telescope with 0°.2 and distance of ∼0°.8 between those two points.

The broad-band energy spectrum is plotted in Fig. 7 along with theoretical predictions (described below). Also in this figure, we plot other data from the ATCA (Australia Telescope Compact Array),³³ ASCA^{25,30} and EGRET. The upper limit of GeV gamma rays in this region was derived from the EGRET archival data.¹

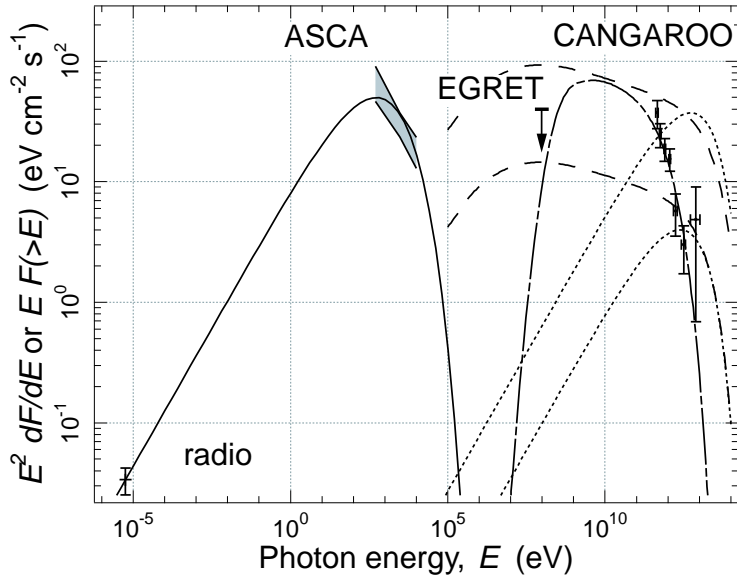


Figure 7: Multi-band emission of RX J1713.7-3946 with models. The TeV gamma-ray points are from this work. Lines show model calculations: synchrotron emission (solid line), Inverse Compton emission (dotted lines), bremsstrahlung (dashed lines) and emission from π^0 decay (dot-dashed line).

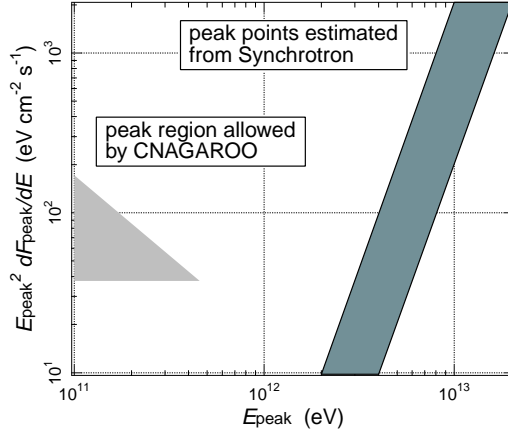


Figure 8: Allowed regions in parameter space (peak in the $E^{**2} dF/dE$ predicted for Cangaroo-II versus the peak position in energy) for the synchrotron-IC model of RX J1713.7-3946. The triangular region on the left side is consistent with the Cangaroo observation while the wide strip on the right side is allowed for the synchrotron-IC model.

In order to explain the broad-band spectrum, three mechanism, (the synchrotron/IC process, bremsstrahlung, and π^0 decay produced by proton-nuclear collisions) are considered. The resultant best fit is plotted in Fig. 7 (the solid line), of which the details are mentioned in Ref.²⁸ We initially assumed the 2.7 K CMB to be seed photons for IC scattering. The calculated inverse Compton Spectra are plotted with dotted lines in Fig. 7 for two typical magnetic field strengths, 3 and $20\mu\text{G}$. Note that these models are far from consistent with the observed sub-TeV spectrum. In general synchrotron/IC process gives a clear correlation between the peak fluxes and its energies of synchrotron and IC emissions as a function of the strength of the magnetic field. We investigated the allowed region of the peak flux of IC emission while taking into account the uncertainties of IR emission for the IC seed photons. The hatched area in Fig. 8 is a theoretically allowed region of the peak flux. Also, an experimentally allowed region is plotted by the shaded area. The predictions of synchrotron/IC models are obviously inconsistent with the experimental data by an order of magnitude.

The bremsstrahlung spectrum was also calculated while assuming that it occurs in the same region as the synchrotron radiation. A material density of ~ 300 protons/cm³ was assumed. The dashed lines in Fig. 7, for magnetic fields of 3 and $20\mu\text{G}$, are both inconsistent with our observation. In the bremsstrahlung process, high-energy electrons also ionize a neutral atom in the plasma, and hence 6.4 keV line emission of neutral ions is expected to be observed simultaneously. However, the observed X-ray spectra from any position of this SNR shows no peak at around 6.4 keV, which also indicates that bremsstrahlung is not dominant in the gamma-ray emission.

Thus, electron-based models fail to explain the observational results. We then examined π^0 decay models. The π^0 s are produced in collisions of accelerated protons with the interstellar matter. A model³⁴ adopting Δ -resonance and scaling was used, considering plausible parameter regions of typical shock acceleration theory. The result is shown by the dot-dashed curve in Fig. 7. The best-fit parameters for the total energy of accelerated protons (E_0) and matter density (n_0) must satisfy $(E_0/10^{50}[\text{ergs}]) \cdot (n_0[\text{protons}/\text{cm}^3]) \cdot (d/6[\text{kpc}])^{-2} = 300$, where d is the distance to RX J1713.7-3946. A value of $E_0 \sim 10^{50}[\text{ergs}]$ gives n_0 on the order of 10 or 100[protons/cm³] for distances of 1 or 6 kpc, respectively. Both cases look consistent within the plausible molecular column density. Thus, the π^0 -decay model alone readily explains our results, which provides the first observational evidence that protons are accelerated in SNR to at least TeV energies. The details are described in a published paper.²⁸

After this publication, several counterarguments have been presented; those argued

that the gamma-ray spectrum calculated from our data using the proton acceleration model conflicts with the upper limit of EGRET in the GeV region.^{35,36} Figure 9 shows the several possible gamma-ray spectra expected from the proton acceleration model by varying the index of the power law of accelerated protons within a reasonable range. In addition, the error region of our data is plotted. There remains the possibility of the proton acceleration model. What we pointed out here is that Synchrotron IC model is very difficult to explain both X-ray and TeV gamma-ray spectra. Thus, our data inductively support the proton acceleration model. Recently, Uchiyama et al, analyzed the Chandra data, and their result also supports our conclusion.³⁷ Furthermore, a recent CO observation with a good angular resolution from the NANTEN observatory³⁸ shows two important results concerning this argument. One is a good coincidence with the TeV gamma-ray emission region and one of dense CO clouds surrounding this SNR; the other is that the distance to the SNR has been found to be 0.9 kpc, while an EGRET object near to this SNR is about 6 kpc, based on a measurement of the velocity of CO. These results further support our conclusion.

5 Summary

More detections of TeV gamma rays from SNR's will obviously advance studies of the Galactic cosmic-ray origin and the shock acceleration mechanism with multi-wavelength observations for SNR's. In particular, the combination of morphological studies in both X-rays and gamma-rays will be a key factor. Advanced X-ray telescope satellites, Chandra and Newton, are now providing excellent images and spectroscopy of many SNR's. Also, stereo observations by the 10m-class Air Čerenkov telescopes will soon provide good quality TeV gamma-ray images with an angular resolution of ≤ 0.1 degree,³⁹ and cover a wide energy range from 0.1 to near 100 TeV. In the southern hemisphere, the CANGAROO⁴⁰ (Fig. 10) and H.E.S.S⁴¹ groups began the stereo observations using 10m-class IACTs in 2003.

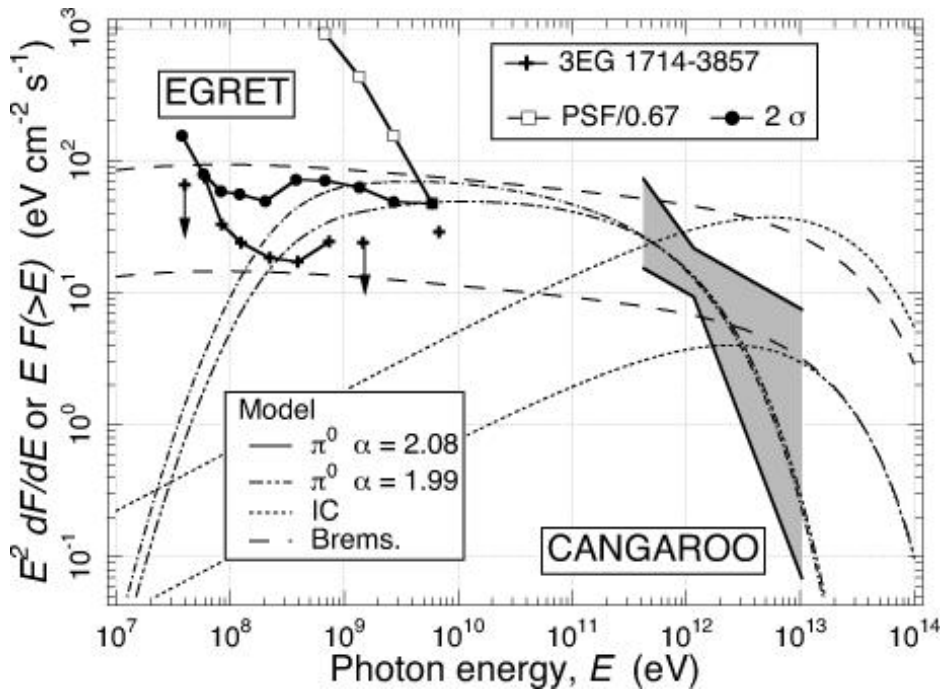


Figure 9: Revised expected gamma-ray spectra of RX J1713.7-3946 based on the models. The observed TeV gamma-ray points are the same as that in the publication, while the error band is added. A differential upper limits in the GeV region was estimated using the EGRET archived data. Lines show model calculations: Inverse Compton emission (dotted lines), bremsstrahlung (dashed lines) and emission from π^0 decay (dot-dashed lines) which were calculated for two reasonable power indices of accelerated protons.



Figure 10: Three 10m telescopes in the CANGAROO site in November 2002.

References

- [1] R.C. Hartmann *et al.*, *Astrophys. J. Suppl.*, 123, 79, (1999)
- [2] T. C. Weeks *et al.*, *Astrophys. J.*, 342, 379, (1989)
- [3] M. Punch *et al.*, *Nature*, 358, 477, (1992)
- [4] J. Quinn *et al.*, *Astrophys. J.*, 456, L85, (1996)
- [5] T. Kifune *et al.*, *Astrophys. J.*, 438, L91, (1995)
- [6] A.M, Hillas, *Proc. 19th Int. Cosmic-Ray Con.*(La Jolla), 3, 445, (1985)
- [7] T. Hara *et al.*, *Nucl. Instrum. Methods Phys. Rev.*, A332, 300, (1993)
- [8] T.C. Weekes, *Proc. of GeV-TeV Gamma Ray Astrophysics Workshop* (Snowbird), ed B. Dingus, 3
- [9] T. Tanimori *et al.*, *Astrophys. J.*, 497, L25, (1998)
- [10] H. Muraishi *et al.*, *Astron. Astrpophys.*, 354, L57, (2000)
- [11] F. Aharonian *et al.*, *Astron. Astrpophys.*, 370, L12, (2001)
- [12] C. Itoh *et al.*, *Astron. Astrpophys.*, 396, L2, (2002)
- [13] L.O'C. Drury, W.J. Markiewicz and W.J. Volk *Astron. Astrpophys.*, 225, 179, (1989)
- [14] R.D. Blandford and D. Eichler, *Phys. Rep.*, 154, 1, (1987)
- [15] L.I. Sedov, *Similarity and Dimensional Methods in Mechanics* (Academic Press, 1959).
- [16] G. B. Rybichi and A. P. Lightman, *Radiation Processes in Astrophysics*, (John Wiley and Sons, 1979), and references therein.
- [17] K. Koyama *et al.*, *Nature*, 376, 255, (1995)
- [18] M. Pohl, *Astron. Astrpophys.*, 307, L57, (1996)
- [19] A. Mastichiadis, *Astron. Astrpophys.*, 305, L53, (1996)
- [20] A. Mastichiadis and O.C. Jager, *Astron. Astrpophys.*, 311, L5, (1996)
- [21] T. Yoshida and S. Yanagita *Proc. 2nd INTEGRAL Workshop*, ESA SP382, 85, (1997)
- [22] S. Hara *et al.*, *et al.*, *Proc. 27th Int. Cosmic-Ray Con.*(Hamburg), 6, 2455, (2001)
- [23] T. Naito *et al.*, *Astron. Nachr.*, 320, 205, (1999)
- [24] R. Willingale *et al.*, *Mon. Not. R. Astron. Soc.*, 278, 749, (1996)

- [25] K. Koyama *et al.*, *Publ. Astron. Soc. Japan*, 49, L7, (1997)
- [26] P. Slane *et al.*, *Astrophys. J.*, 525, 357, (1999)
- [27] T. Tanimori *et al.*, *Proc. 27th Int. Cosmic-Ray Con.*(Hamburg), 6, 2465, (2001)
- [28] R. Enomoto *et al.*, *Nature*, 416, 823, (2002)
- [29] T. Tanimori *et al.*, *Proc. on 27th ICRC2001*, 6, 2465, (2001)
- [30] H. Tomida, *Synchrotron Emission from the Shell-like Supernova Remnants and the Cosmic-Ray Origin*, Ph. D. thesis, Kyoto Univ. (1999)
- [31] Skyview, see <http://skyview.gsfc.nasa.gov>
- [32] Y. M. Butt *et al.*, *Astrophys. J.*, 562, L167, (2001)
- [33] D. C. Ellison, P. Slane, and B. M. Gaensler, *Astrophys. J.*, 563, 191, (2001)
- [34] T. Naito and F. Takahara, *J. Phys. G*, 20, 477, (1994)
- [35] O. Reimer and M. Pohl, *Astron. Astrophys.*, 390, L43, (2002)
- [36] M. Butt *et al.*, *Nature* 418, 489, (2002)
- [37] Y. Uchiyama, F. Aharonian, and T. Takahashi, *Astron. Astrphys.*, 400, 567, (2003)
- [38] Y. Fukui *et al.*, *Publ. Astro. Soc. of Japan* Vol 55, L61 (2003)
- [39] R. Enomoto *et al.*, *Astropart. Phys.* 16, 235, (2002)
- [40] see <http://icrhp9.icrr.u-tokyo.ac.jp>
- [41] see <http://www.mpi-hd.mpg.de/hfm/HESS>